Korean J. Chem. Eng., 40(12), 2815-2825 (2023)
DOI: 10.1007/s11814-023-1574-0

pISSN: 0256-1115
eISSN: 1975-7220

Elevated energy efficiency and reduced CO_2 emissions from integrated reaction and separation for the concurrent production of ethers

Jeongwoo Lee, Minyong Lee, Donggun Kim, Yongbeom Shin, and Jae W. Lee†

Department of Chemical and Biomolecular Engineering, Korea Advanced Institute of Science and Technology (KAIST), 291 Daehak-ro, Yuseong-gu, Daejeon 34141, South Korea
(*Received 4 August 2023 • Revised 4 September 2023 • Accepted 5 September 2023*)

Abstract−This study aimed to design energy-efficient systems for reactive distillation to simultaneously produce methyl tert-butyl ether (MTBE) and ethyl tert-butyl ether (ETBE) from mixed feeds of methanol and ethanol. In this work, two new designs are proposed. One is the individual production of each ether, involving two reactive distillation columns after feed alcohol separation, while the other for the co-production of both ethers in a single reactive distillation column without the alcohol separation. Rigorous simulations of the two proposed systems were conducted with varying ratios of the two alcohols in actual process streams. When the methanol feeding was dominant, the co-production system exhibited better performance than the individual ether production system. This was due to the lower temperatures inside the alcohol separation column, resulting in a lower relative volatility of methanol and increasing the heat duty in the alcohol separation column. However, when the amount of ethanol was higher than that of methanol, the individual production system outperformed the co-production system. This was attributed to the unfavorable reaction equilibrium of ETBE production, leading to a high internal flowrate in the co-production reactive distillation column. The external heat integration of each design can bring further reduction in energy consumption and CO_2 emissions, but the results follow the same dependence on the feed alcohol ratio.

Keywords: Concurrent Production, Process Intensification, Reactive Distillation, Energy Efficiency, CO_2 Emission

INTRODUCTION

Distillation is a key separation process in the chemical industry for obtaining highly pure products. However, this process is energy intensive and produces significant greenhouse gas emissions [1,2]. Therefore, previous studies [3,4] have focused on designing methods to reduce CO_2 emissions and energy consumption for this separation process, in a similar way to approaches used for other interphase mass-transfer units [5,6]. Reactive distillation (RD), a process intensification technique, combines both chemical reaction and separation [7,8]. An RD system offers several advantages, including the ability to circumvent azeotropes by depleting the reactant responsible for their formation [9,10], economic benefits due to fewer operational units [11,12] and reduced CO_2 emissions through lower energy consumption [13,14]. Furthermore, the continuous removal of products in RD systems leads to a shift in chemical equilibrium [15,16]. Therefore, this technique has been applied to various equilibrium-limited reactions, such as esterification and etherification [17, 18].

Research has been conducted on the application of the etherification reaction in RD systems. In particular, studies have focused on RD systems for the production of methyl tert-butyl ether (MTBE) and ethyl tert-butyl ether (ETBE). Previous studies implemented the residue curve map of MTBE and ETBE production systems to propose designs for RD columns [19,20]. In addition to RD column design, earlier work also introduced heat integration (HI) into the MTBE and ETBE production RD systems to augment thermodynamic and energy efficiency [21,22]. These oxygenated fuel additives serve as octane rating enhancers and antiknock agents, replacing lead-containing materials [23-25].

Other studies have been conducted on RD systems that simultaneously produce multiple targeted products using common reactants [12,26]. For example, MTBE and ETBE are both produced from the common reactant, isobutene (IB), while the alcohol reactant varies. However, there have been no studies on RD systems that produce MTBE and ETBE simultaneously within the same system. In addition, if the reactant stream contains different alcohol feed compositions, the economic feasibility of the proposed RD system can vary according to the alcohol feed ratios. The mixed feed of methanol (MeOH) and ethanol (EtOH) can derive from the hydrogenation of CO_2 [27], the thermochemical conversion of glycerol [28], pharmaceutical plants, and semiconductor industries [29,30]. From such processes, the ratio of MeOH to EtOH produced can be wide-ranging (from 104.9 to 0.003) [27]. Therefore, it is necessary to evaluate different column sequence alternatives for the RD design when we simultaneously produce MTBE and ETBE with mixtures of MeOH and EtOH by considering their varying feed ratios. This dependence of feed compositions on the design is underinvestigated. Therefore, this study investigated RD systems for the simultaneous production of MTBE and ETBE while considering changes in the feed composition.

Thus, in this study, new RD-based systems called co-production

†To whom correspondence should be addressed.
E-mail: jaewlee@kaist.ac.kr

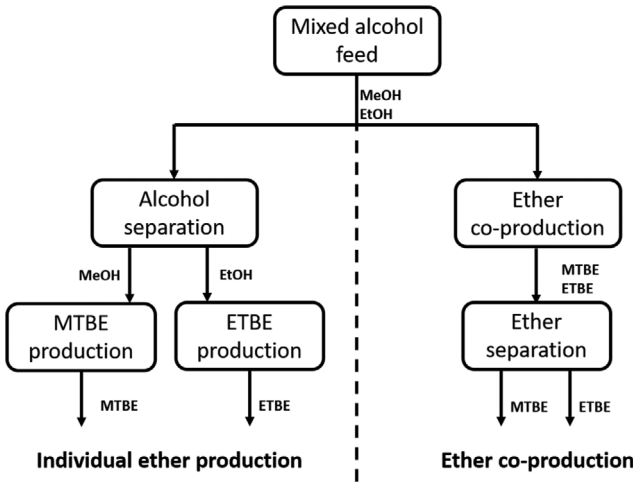

Fig. 1. Two RD design sequences of individual ether production and ether co-production system.

and individual production system, which produces both MTBE and ETBE simultaneously, are proposed. Here, these two sequences with external HI were also considered: one involves the individual production of MTBE and ETBE in each respective RD column, with the reactants of MeOH and EtOH being separated and pure alcohols used as feeds; the other sequence involves the simultaneous production of MTBE and ETBE in a single RD column, using a mixed alcohol feed, as shown in Fig. 1. Different feed ratios of MeOH to EtOH were employed in each RD system. To evaluate the designed systems, energy consumption, economic feasibility, and CO_2 emission rates were compared. In addition, external HI was applied into the both systems to design energy-efficient, economical, and environmental-friendly systems. The constructed systems were rated and compared with the non-HI systems.

PHYSICAL PROPERTIES AND REACTION KINETIC MODEL

The two fuel ethers, MTBE and ETBE, were synthesized through the etherification reaction of alcohol and IB, with n-butene (NB) present as an inert feed in this system. The reactions using MeOH and EtOH were undertaken using the ion-exchange resin catalyst, Amberlyst 15. Kinetic models for both reactions are based on the activity, denoted by a_i. The reaction kinetic equations [31] and equilibrium constant [32] for MTBE production are given as:

$$\mathrm{MeOH + IB \underset{k_{rate,-1}}{\overset{k_{rate,1}}{\leftrightarrow}} MTBE} \tag{1}$$

$$r_{MTBE} = \frac{dC_{MTBE}}{dt} = m_{cat} q k_{rate,1}\left(\frac{a_{IB}}{a_{MeOH}} - \frac{a_{MTBE}}{K_{eq,1} a_{MeOH}^2}\right) \tag{2}$$

$$k_{rate,1} = 243.8 \times 10^{-3} \exp\left(-\frac{92400}{R}\left[\frac{1}{T} - \frac{1}{363.15}\right]\right) \tag{3}$$

$$K_{eq,1} = \exp\left(-10.10 + \frac{4254}{T} + 0.2667 \ln(T)\right) \tag{4}$$

where m_{cat} is the amount of catalyst (kg), and q is the amount of acid groups on the resin per unit mass (4.9/kg). $k_{rate,1}$ is the forward reaction rate constant (mol/s/kg). The reverse reaction rate constant, $k_{rate,-1}$, is determined by the forward reaction rate constant ($k_{rate,1}$) and equilibrium constant ($K_{eq,1}$) with the amount of catalyst (m_{cat}) in $m_{cat} q \frac{k_{rate,1}}{K_{eq,1}}$.

The ETBE reaction kinetic equations and equilibrium constant are given as [33]:

$$\mathrm{EtOH + IB \underset{k_{rate,-2}}{\overset{k_{rate,2}}{\leftrightarrow}} ETBE} \tag{5}$$

$$r_{ETBE} = \frac{dC_{ETBE}}{dt} = m_{cat} k_{rate,2}\left(\frac{a_{IB}}{a_{EtOH}} - \frac{a_{ETBE}}{K_{eq,2} a_{EtOH}^2}\right) \tag{6}$$

$$k_{rate,2} = 1.209 \times 10^{12} e^{-87200/RT} \tag{7}$$

$$K_{eq,2} = \exp\left(10.39 + \frac{4061}{T} - 2.891 \ln(T) - 0.0192T + 5.286 \times 10^{-5} T^2 - 5.330 \times 10^{-8} T^3\right) \tag{8}$$

To determine the vapor-liquid equilibrium (VLE), the UNIQUAC activity coefficient model, which was previously studied for each fuel ether production system [31,34], was used. For the missing binary parameters in the Aspen Plus® databank, UNIFAC estimation was employed to predict the VLE. The binary interaction parameters are given in the Supplementary Information (refer to Table S1). Using these binary interaction parameters, the results of the singular point analysis at a RD column pressure of 9.5 atm are displayed in Table 1.

Table 1. Result of the singular point analysis in 9.5 atm

Singular points	Temp (°C)	Classification
NB 91.9%+MeOH 8.1%	67.744	Unstable node
IB 93.8%+MeOH 6.1%	68.741	Saddle
NB 90.5%+IB 9.5%	69.093	Saddle
NB	69.097	Saddle
IB	69.464	Saddle
MeOH 59.0%+MTBE 41.0%	128.536	Saddle
ETBE 24.9%+MeOH 75.1%	131.213	Saddle
MeOH	135.328	Saddle
EtOH 42.6%+MTBE 57.4%	137.421	Saddle
ETBE 22.4%+EtOH 77.6%	141.845	Saddle
MTBE	146.046	Saddle
EtOH	149.356	Stable node
ETBE	166.844	Stable node

SYSTEM DESCRIPTION AND EVALUATION

The column pressure has a significant effect on the reaction as well as energy consumption, so it is set before the optimization of each column. Typically, RD columns for MTBE and ETBE production are operated within a high-pressure range of 8-10.95 atm [32, 35,36]. Therefore, the overhead pressure of the RD column was maintained at 9.5 atm to ensure it falls within the pressure range for both ether production reactions. The overhead pressure of the non-reactive column for each fuel ether separation column and

alcohol separation column was set to 1 atm.

In both the individual production and co-production systems for the ethers, a pre-reactor is introduced before the RD column to increase the alcohol conversion. The same ion-exchange resin catalyst is utilized in the pre-reactor. A continuous stirred tank reactor model was used for the simulation, and the design specifications of the pre-reactor were adopted from the previous study [37].

The alcohol feed ratio was varied while maintaining the IB and NB feed flowrate constant to assess the flexibility of the system. The alcohol feed was slightly in excess (alcohol : IB=1.005 : 1) compared to the reactant IB feed so that the side dimerization reaction of IB was ignored [38]. Also, by maintaining the same IB and NB feed flowrate in all cases, the total target ether product flowrate remained the same. Several case studies were conducted with different alcohol feed ratios (MeOH : EtOH=3.5 : 1, 3 : 1, 2 : 1, 1 : 1, 1 : 2, 1 : 3, 1 : 3.5), and among them, three cases (3.5 : 1, 1 : 1, 1 : 3.5) were selected as representatives for discussion. Using various alcohol feed mixtures, the individual production system and the co-production system were simulated and assessed. For the distillation and RD columns, iterative optimization (refer to Fig. S1 in the Supplementary Information) [39] was performed while ensuring the molar purity of the fuel ethers remained above 99.5 mol%.

1. Individual Fuel Ether Production

Individual MTBE and ETBE RD systems are capable of achiev-

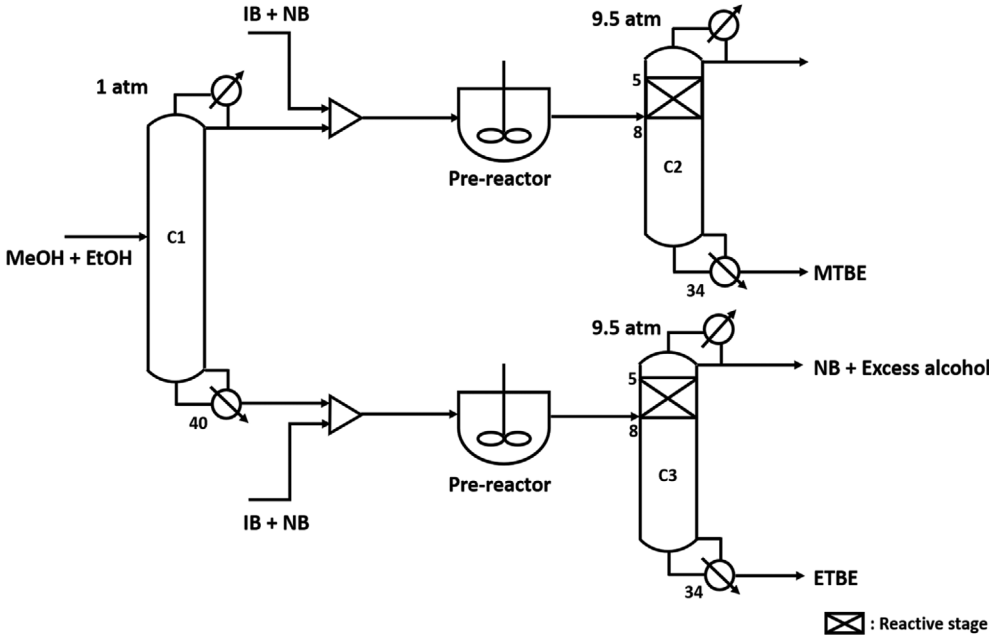

Fig. 2. Flowsheet of the individual fuel ether production system.

Table 2. Individual production simulation results

MeOH : EtOH	3.5 : 1	1 : 1	1 : 3.5
Alcohol feed flowrate [kmol/hr]	131.41	131.41	131.41
Total C4 feed flowrate [kmol/hr] (IB : NB=0.560 : 0.440)	233.49	233.49	233.49
C1			
Feed stage	27	26	22
Flowrate of distillate/bottom [kmol/hr]	102.208/29.202	65.705/65.705	29.203/102.21
Temperature of distillate/bottom [°C]	64.56/84.37	64.57/84.40	64.58/84.44
C2			
Flowrate of distillate/bottom [kmol/hr]	80.709/101.98	51.549/65.461	22.950/29.083
Temperature of distillate/bottom [°C]	67.99/146.75	67.92/146.89	67.82/146.94
Product purity of bottom	0.995	0.995	0.995
C3			
Flowrate of distillate/bottom [kmol/hr]	22.974/29.128	51.452/65.558	80.184/101.93
Temperature of distillate/bottom [°C]	70.74/167.71	70.82/167.69	70.97/167.67
Product purity of bottom	0.995	0.995	0.995

ing full conversion of the key reactant and recovering pure ether products, because each ether product represents a stable node in the distillation diagram and is continuously removed as a bottom product of the RD column [40,41]. The design sequence of individual fuel ether production consists of three columns: a MeOH/EtOH separation column and two RD columns for MTBE and ETBE production, with a pre-reactor located between the columns (Fig. 2). The mixed alcohols are separated into MeOH (top product) and EtOH (bottom product) using the non-reactive separation column. The C4 (IB and NB) stream is introduced to each reactor after the alcohol separation. The inert NB is withdrawn as the top stream in each ether production RD column along with excess alcohols. MTBE and ETBE, which has higher boiling points than NB, are separated as the bottom stream in each fuel ether production column. The corresponding stream results of the individual production system are shown in Table 2.

2. Fuel Ether Co-production

The co-production RD system for MTBE and ETBE was able to obtain high purity ethers. The alcohol flowrate was slightly in excess compared with IB, and a binary mixture of MTBE and ETBE products was continuously removed from the bottom of the RD column. The limiting common reactant, IB, was completely consumed in the pre-reactor and RD column, and any azeotropes involving IB were eliminated, having no impact on the vapor and liquid separation. The ether co-production system consisted of one pre-reactor and two columns: one RD column for ether co-production and another non-reactive column for ether separation. Unlike the previous individual ether production system, there was no separation column for the mixture alcohol. After MTBE and ETBE were produced by the pre-reactor, the unconverted reactant stream was fed into the intensified RD column for the co-production of MTBE and ETBE. The inert NB, along with excess alcohols, was withdrawn from the top of the ether co-production RD column. The product mixture of MTBE and ETBE at the bottom of the RD column was separated in the non-reactive ether separation column, as shown in Fig. 3.

The reactive stage profiles of RD column reveal a low alcohol composition near the feed stage. In the case of MeOH : EtOH= 1 : 1, the liquid composition profile of the RD column is shown in Fig. 4 (for the other cases, refer to Fig. S2). This suggests that the majority of the reaction occurs around the feed stage. Through the reactions in the pre-reactor and the RD column, high purities and product recovery were achieved, and the stream results of the co-production system are shown in Table 3.

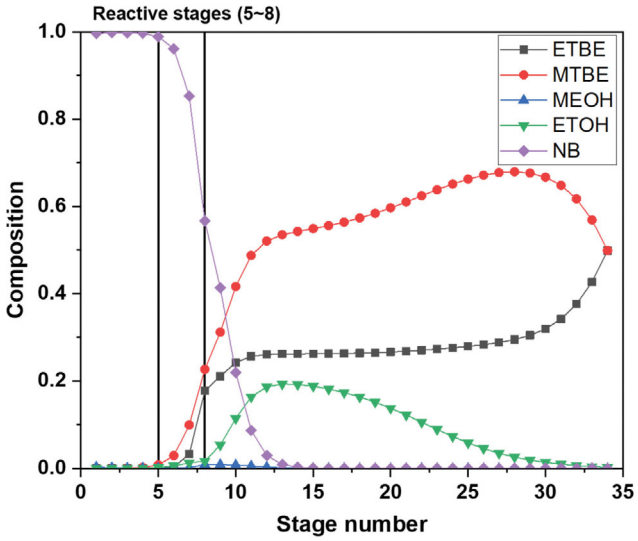

Fig. 4. Liquid phase profile of the fuel ether co-production column in the case of MeOH : EtOH=1 : 1.

3. Energy, Economic, and CO_2 Emission Assessment

3-1. Energy Comparison

For the energy usage of each case, total utility consumption (TUC) is evaluated for all cases. TUC is calculated with the following equation:

$$TUC = \Sigma_i Q_{reb} - \Sigma_i Q_{cond} + \Sigma Q_{other} \quad (9)$$

where Q_{reb} refers to the heat duty of reboiler, Q_{cond} is the heat duty of condenser and it has a negative sign, and Q_{other} denotes the heat

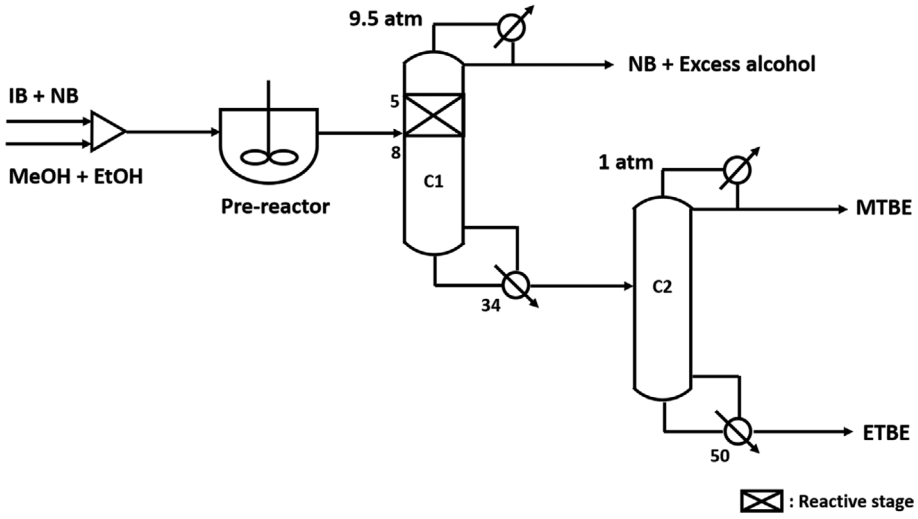

Fig. 3. Flowsheet of fuel ether co-production system.

Table 3. Co-production simulation results

MeOH : EtOH	3.5 : 1	1 : 1	1 : 3.5
Alcohol feed flowrate [kmol/hr]	131.41	131.41	131.41
Total C4 feed flowrate [kmol/hr] (IB : NB=0.560 : 0.440)	233.49	233.49	233.49
C1			
Flowrate of distillate/bottom [kmol/hr]	103.80/129.71	103.19/130.96	103.35/130.80
Temperature of distillate/bottom [°C]	67.98/151.11	68.93/156.31	68.72/158.15
C2			
Flowrate of distillate/bottom [kmol/hr]	100.66/29.052	65.315/65.641	28.636/102.16
Temperature of distillate/bottom [°C]	55.04/81.84	55.03/81.83	55.03/81.89
Product purity of distillate/bottom	0.995/0.995	0.995/0.995	0.995/0.995

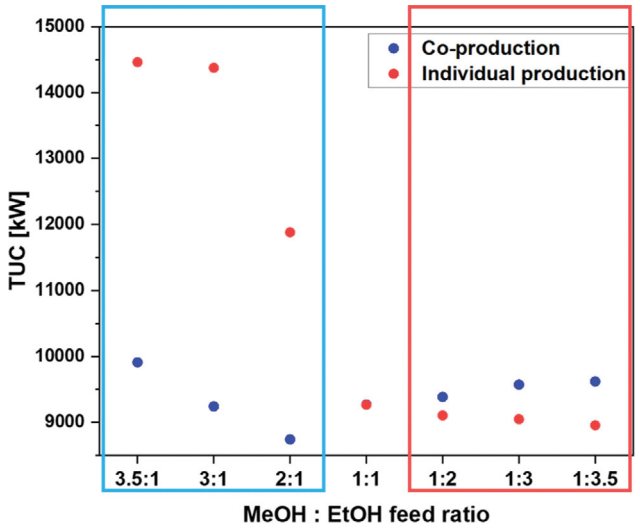

Fig. 5. TUC comparison of co-production system and individual production system (blue box: MeOH excess cases, red box: EtOH excess cases).

duty of the pump or auxiliary heater (in the external HI system).

Fig. 5 shows the TUC comparison results for the individual production and co-production systems (also refer to Table S2). When MeOH : EtOH=3.5 : 1, the TUC of the co-production system is reduced by 31.5% compared to the individual system. However, no significant difference in TUC is observed when the MeOH and EtOH flowrates are equal (note that the case with a 1 : 1 feed ratio in Fig. 5 has overlapping blue and red circles). In the remaining cases, the individual production system shows lower energy consumption than the co-production system. In the case of MeOH : EtOH=1 : 3.5, the co-production system exhibits a higher TUC of 9.29% compared to the individual system. This disparity is due to differences in utility consumption in the alcohol separation column (refer to Table S3).

The alcohol separation column in the individual production system requires a significant amount of energy. Of the overall energy consumption of the individual production system, the alcohol separation column energy consumption accounts for 79.2%, 73.0%, and 64.0% when MeOH : EtOH=3.5 : 1, 1 : 1, 1 : 3.5, respectively (refer to Table S4-S6). When the amount of MeOH is higher than

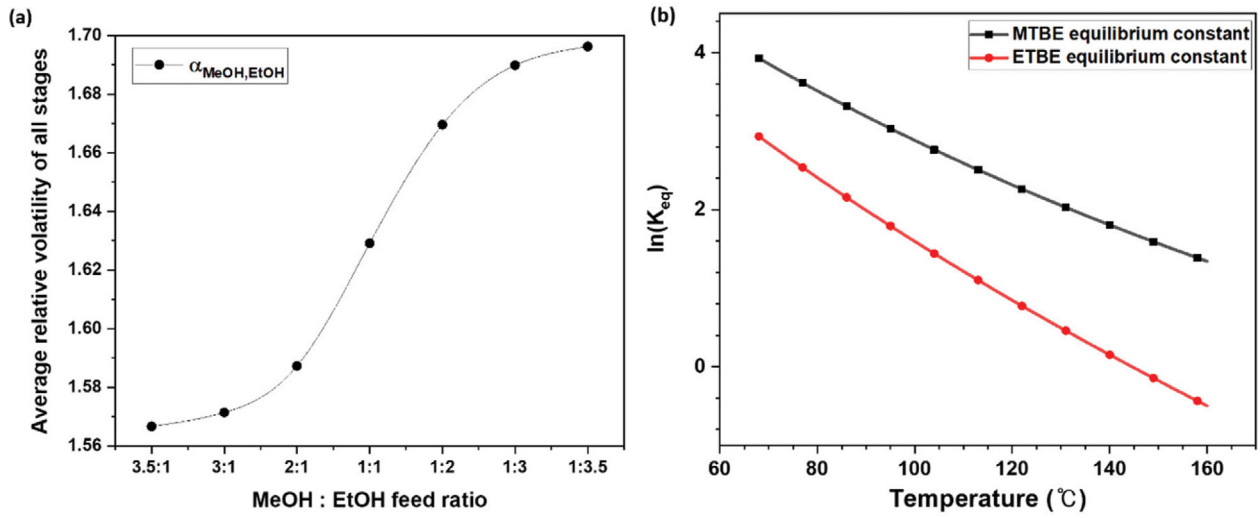

Fig. 6. (a) Average relative volatility of alcohol separation column in different alcohol feed ratios; (b) Comparison of reaction equilibrium constant between MTBE and ETBE.

that of EtOH in the feed, the internal temperature of the alcohol separation column decreases due to the low boiling point of MeOH. This leads to a decrease in the relative volatility of the alcohol separation column, as shown in Fig. 6(a). Referring to a previous study [42], low relative volatility exhibits poor separation efficiency, requiring more stages or higher heat duty. Therefore, more heat is required in cases where MeOH is in excess. Fig. 6(a) displays the average relative volatility of all stages in the alcohol separation column, clearly demonstrating that as the amount of EtOH increases, the relative volatility between MeOH and EtOH increases, resulting in easier separation and reduced energy consumption (refer to Table S3). In the co-production system, a large amount of ETBE shows higher volatility, so lower heat duty is required for the fuel ether separation column in the case of EtOH-dominant feed. However, in the RD column operating temperature range of 68-159 °C, the equilibrium constant of the ETBE reaction is smaller than that of MTBE, as shown in Fig. 6(b). Since high internal flow is required for a higher reaction conversion of EtOH, the reflux ratio of the RD column increases when the EtOH amount increases (refer to Table S7). Therefore, a larger amount of energy is required in the co-production RD column for the EtOH-dominant feed as shown in Fig. 5.

3-2. Economic Comparison

Total annual cost (TAC), which includes capital and operating costs, can be calculated by using the following equation [45]:

$$\text{TAC} = \frac{\text{Total capital cost (\$)}}{\text{Payback period (yr)}} + \text{Total operating cost (\$/yr)} \quad (10)$$

The operating cost mainly consists of steam utility, cooling water, and electricity. The capital cost includes, among other things, column vessel costs, heat exchanger costs, and installation costs. Due to the relatively low-cost ratio compared to other pieces of equipment, the costs of common pumps and pipelines were not included in the calculation for all cases. It was assumed that the operating time is 8,000 hours per year and the payback period was three years. The capital cost, utility type, and operating cost were calculated (refer to Table S8).

Concurrently with the TUC trend in Fig. 5, the total operating cost and TAC were lower in the MeOH excess case for the co-production system, while the EtOH excess case showed opposite results as shown in Fig. 7. Since the flowrate and temperature of each stream are similar in all cases, the costs associated with the pre-reactor, column vessel, and heat exchanger are also alike for both systems. Therefore, the TAC is primarily influenced by the operating cost, which mainly depends on the alcohol feed ratio.

When the feed has higher MeOH than EtOH amount, the co-production system exhibits a lower TAC than the individual production system due to the high utility usage in the alcohol separation column. When MeOH : EtOH=3.5 : 1, the co-production system shows a reduced TAC of 27.5% compared to the individual production system. Similar to the TUC results, the difference in TAC between individual production and co-production is barely discernible for the equal feed flowrate of MeOH and EtOH. However, in the case of MeOH : EtOH=1 : 3.5, the TAC of the co-production system increased by 6.43% compared to the individual production system (for all feed ratios, refer to Fig. S3) due to the unfavorable reaction equilibrium of ETBE production, as mentioned before.

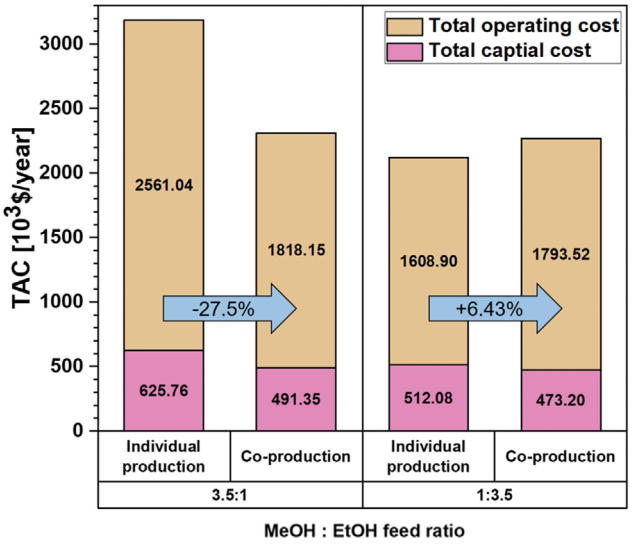

Fig. 7. TAC comparison of the individual production and the co-production system in the case of MeOH : EtOH=3.5 : 1, 1 : 3.5.

3-3. CO_2 Emission Comparison

A large amount of CO_2 is emitted in the distillation system when fossil fuels are combusted or when electricity or steam utility usage is required to meet the temperature requirements. CO_2 emission rates are calculated using a model proposed in previous studies [43-45]. The parameters related to calculation of the CO_2 emission rate are used from a prior work (refer to Table S9) [46]. Fig. 8 depicts the CO_2 emission rate of the individual production and the co-production system for each alcohol feed ratio.

Similar to the findings of the energy comparison and economic evaluation, the CO_2 emission rate was lower when the MeOH feed

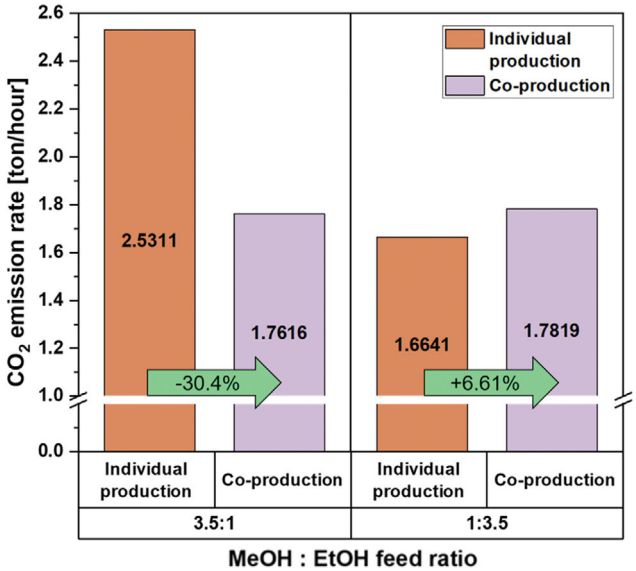

Fig. 8. CO_2 emission comparison of the individual production and the co-production system in the case of MeOH : EtOH=3.5 : 1, 1 : 3.5.

portion was higher than the EtOH feed, and vice versa for the other cases. Due to the high reboiler heat duty in the alcohol separation column when MeOH : EtOH=3.5 : 1, the CO_2 emission rate of the co-production system decreased by 30.4% compared to the individual production system. In the case of MeOH : EtOH=1 : 3.5, the CO_2 emission rate of the co-production system increased by 6.61%. However, no meaningful disparity was observed between the individual and co-production systems in the MeOH : EtOH=1 : 1 case. Therefore, in cases with a higher EtOH feed content, the CO_2 emission rate of the individual production system decreased, while the opposite happened in the co-production system (for all feed ratios, refer to Fig. S4).

HEAT-INTEGRATED SYSTEM DESCRIPTION AND EVALUATION

The external HI method utilizes a heat exchanger between a hot stream and a cold stream to decrease the heat requirement of a reboiler. Introducing an external HI to an RD system can offer additional economic efficiency [47] and reduce CO_2 emissions [48]. Therefore, external HI was performed for the individual production and co-production systems to further decrease TUC, TAC, and CO_2 emissions. In this study, it was assumed that the temperature difference between the hot and cold streams must be greater than 10 K [49]. The constructed systems were then evaluated in respect of the three criteria by using the same model and equations shown in section 3.

1. External Heat-integrated Individual Fuel Ether Production

From the stream temperature data in the individual production scheme, the product streams from both ether production columns can transfer heat to the alcohol separation column as shown in Table 4. By exchanging heat between the low-temperature bottom stream of the alcohol separation column and the high-temperature bottom stream of the ether production column, the energy consumption of the individual ether production systems is reduced. Considering the requirement for a stream with higher heat content to be used as the heat source, the heat capacity of each product stream was calculated and the hot stream was determined (refer to the Supplementary Information and Table S10). Consequently, the MTBE stream was selected as a hot stream in cases with methanol excess, while the ETBE stream was selected as such in the other cases, due to their higher flowrate and transferrable heat. Fig. 9(a) and (b) show the flowsheet of the external HI fuel ether individual production system.

In the results of the inlet and outlet streams of the heat exchanger, the temperature of the cold stream exhibited minimal variation, while the temperature of the hot stream decreased significantly. This is because most of the heat transferred to the cold stream is used for the phase change of the cold stream. Since the recycle stream to the alcohol separation column (indicated by the blue line in Fig. 9(a), (b)) needs to be in the vapor phase, it is necessary to have an auxiliary heater. To obtain high alcohol purity, which directly affects the ether purity, a large recycle flowrate is required.

2. External Heat-integrated Fuel Ether Co-production

From the stream temperature data in the co-production scheme, heat exchange between the two bottom streams in RD and ether separation columns was possible, as shown in Table 5. As high pressure is required for the fuel ether co-production RD column, the temperature of the bottom stream in this column was high enough to provide heat to the reboiler of the fuel ether separation column. Therefore, by incorporating a heat exchanger between the bottom streams of the RD column and the fuel ether separation column, the utility usage of the external HI co-production system is reduced

Table 4. External HI individual production simulation results

MeOH : EtOH	3.5 : 1	1 : 1	1 : 3.5
Alcohol feed flowrate [kmol/hr]	131.41	131.41	131.41
Total C4 feed flowrate [kmol/hr] (IB : NB=0.560 : 0.440)	233.49	233.49	233.49
Cold stream recycle flowrate [kmol/hr]	430.35	451.24	467.79
Outlet cold stream vapor fraction	0.107	0.151	0.184
C1			
Feed stage	27	26	22
Flowrate of distillate/bottom [kmol/hr]	102.208/29.202	65.705/65.705	29.203/102.21
Temperature of distillate/bottom [°C]	64.56/84.37	64.57/84.40	64.58/84.44
C2			
Flowrate of distillate/bottom [kmol/hr]	80.709/101.98	51.549/65.461	22.950/29.083
Temperature of distillate/bottom [°C]	67.99/146.75	67.92/146.89	67.82/146.94
Product purity of bottom	0.995	0.995	0.995
C3			
Flowrate of distillate/bottom [kmol/hr]	22.974/29.128	51.452/65.558	80.184/101.93
Temperature of distillate/bottom [°C]	70.74/167.71	70.82/167.69	70.97/167.67
Product purity of bottom	0.995	0.995	0.995

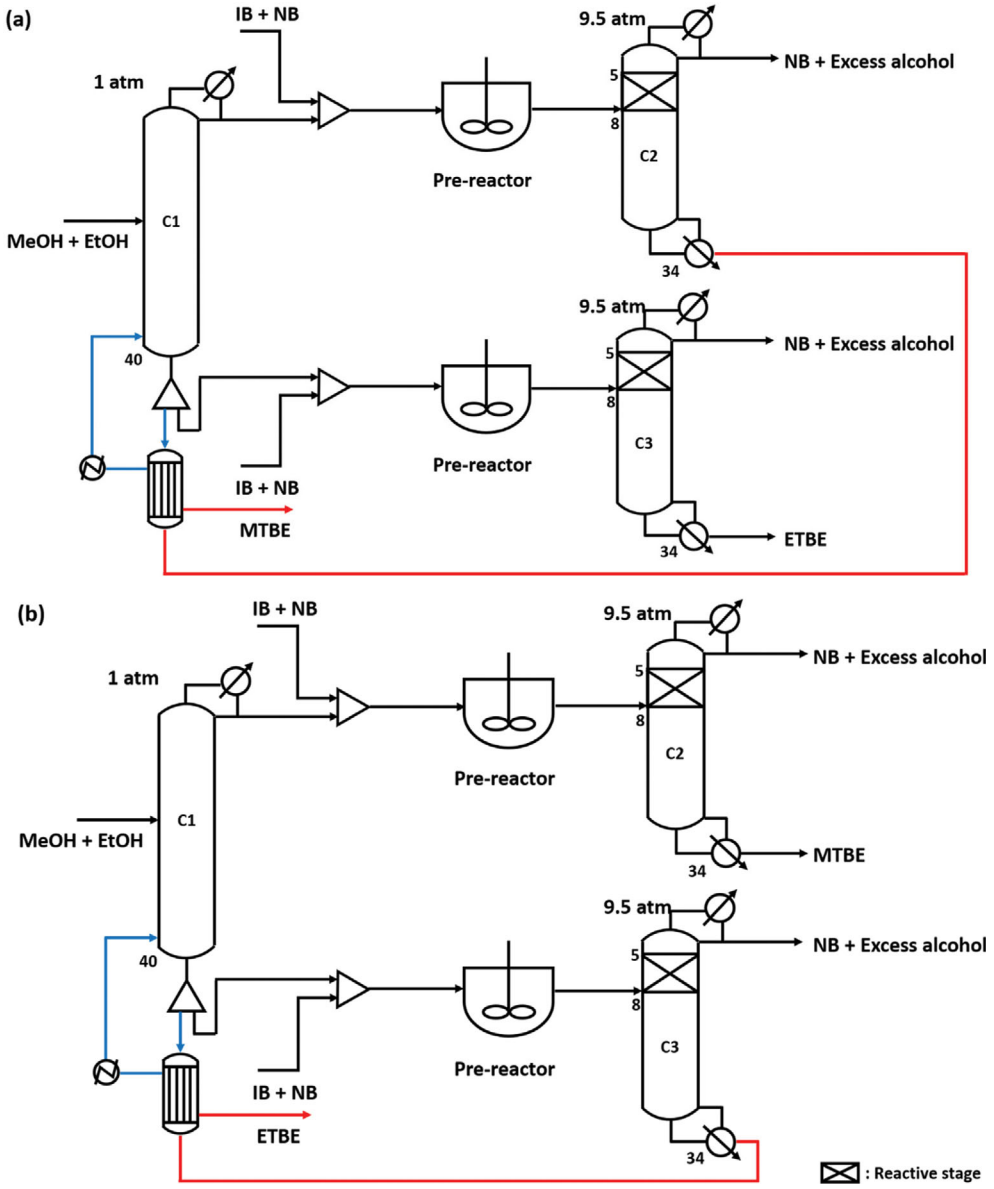

Fig. 9. Flowsheet of external HI fuel ether individual production system (a): Integrating MTBE stream, (b): Integrating ETBE stream.

Table 5. External HI co-production simulation results

MeOH : EtOH	3.5 : 1	1 : 1	1 : 3.5
Alcohol feed flowrate [kmol/hr]	131.41	131.41	131.41
Total C4 feed flowrate [kmol/hr] (IB : NB=0.560 : 0.440)	233.49	233.49	233.49
Cold stream recycle stream flowrate [kmol/hr]	271.62	259.64	240.74
Outlet cold stream vapor fraction	0.284	0.268	0.271
C1			
Flowrate of distillate/bottom [kmol/hr]	103.80/129.71	103.19/130.96	103.35/130.80
Temperature of distillate/bottom [°C]	67.98/151.11	68.93/156.31	68.72/158.15
C2			
Flowrate of distillate/bottom [kmol/hr]	100.66/29.052	65.315/65.641	28.636/102.16
Temperature of distillate/bottom [°C]	55.04/81.84	55.03/81.83	55.03/81.89
Product purity of distillate/bottom	0.995/0.995	0.995/0.995	0.995/0.995

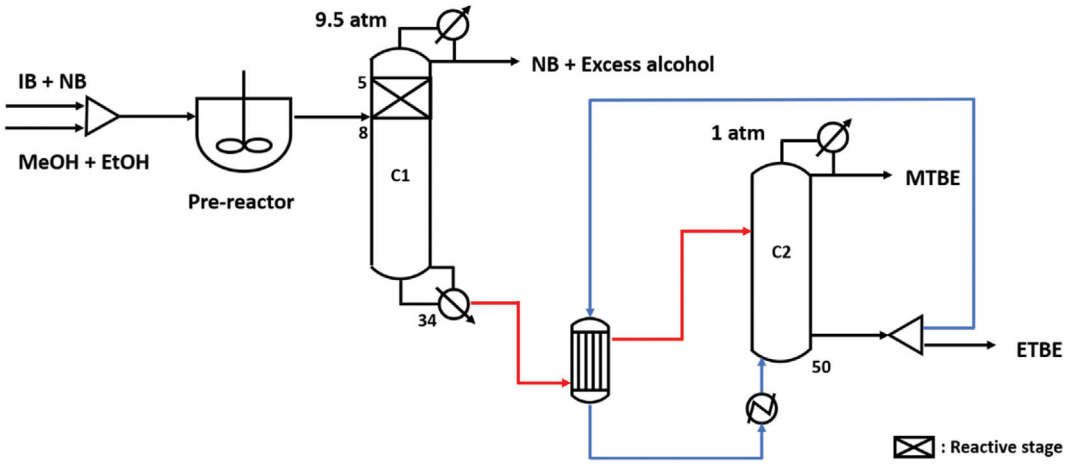

Fig. 10. Flowsheet of external HI fuel ether co-production system.

compared to the bare co-production system. Fig. 10 shows the flowsheet of the external HI fuel ether co-production system.

Introducing the HI method to the ether co-production system leads to a decrease of the hot stream temperature and increases the vapor fraction of the cold stream. An auxiliary heater was utilized to increase the vapor fraction of the recycle stream (indicated by the blue line in Fig. 10) to 1. A significant amount of recycle flowrate is required to meet the purity constraint of the final product.

3. Heat Integrated System Evaluation

3-1. Energy Comparison

In both external HI production systems, heat from the hot stream is transferred to the cold stream, and this heat transfer reduces the reboiler heat duty. Due to the higher flow rate of the hot stream (ETBE product stream) in the external HI co-production system, it is capable of substituting the heat duty of the reboiler with the low recycle flowrate. Therefore, the external HI method is more energy-efficient when applied in the co-production system than in the individual production system. Fig. 11 shows that the TUC is dramatically reduced in the MTBE and ETBE co-production compared to their individual production for the MeOH excess feeds, while the individual production is slightly favorable for the EtOH excess feeds (refer to Table S4-S6 for detailed information of TUC in three cases).

3-2. Economic Evaluation

When the external HI was introduced into the co-production system, it resulted in a greater reduction in TAC compared to its implementation in the individual production system. Due to the decline in the energy requirement when external HI is applied, the required total operating cost decreases. Consequently, the external HI applied systems were more economically feasible compared to the bare systems. In the case of MeOH : EtOH=3.5 : 1 and 1 : 3.5, the TAC of the external HI co-production system decreased by

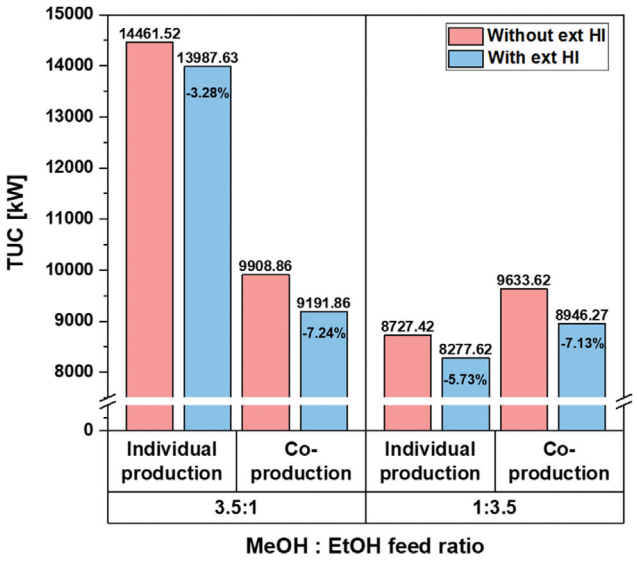

Fig. 11. TUC comparison between the systems with and without external HI method in MeOH : EtOH=3.5 : 1 and 1 : 3.5.

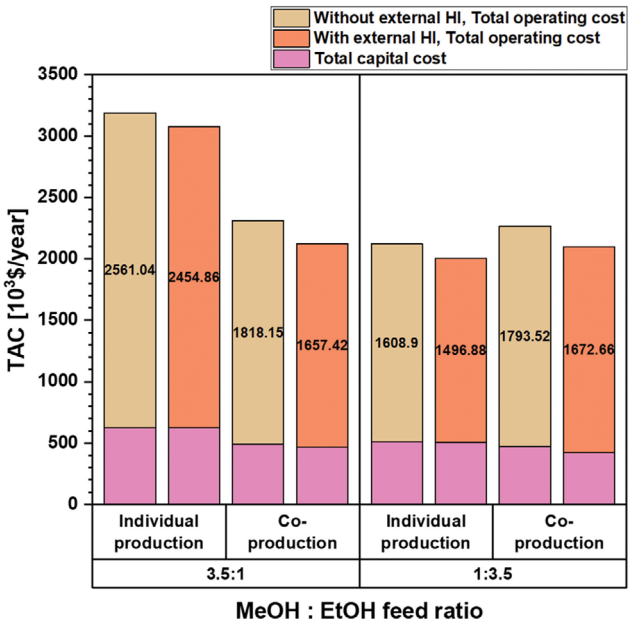

Fig. 12. TAC comparison between the systems with and without external HI method in MeOH : EtOH=3.5 : 1 and 1 : 3.5.

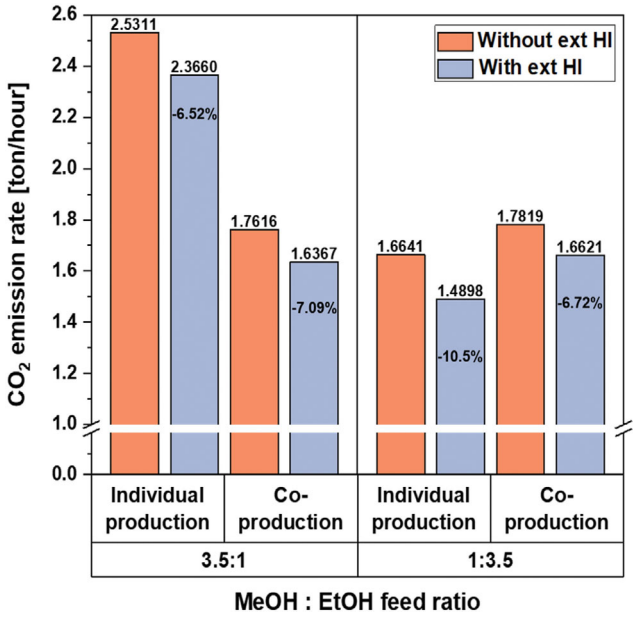

Fig. 13. CO_2 emission comparison between the systems with and without external HI method in MeOH : EtOH=3.5 : 1 and 1 : 3.5.

8.05% and 7.51%, respectively, compared with the bare co-production system. Similarly, for the HI of the individual production system, the TAC decreased by 3.43% and 5.48% in the respective cases, as shown in Fig. 12.

3-3. CO_2 Emission Evaluation

The external HI decreases the reboiler heat duty of the separation column, and this leads to a lower CO_2 emission rate, as shown in Fig. 13. For the co-production system, the external HI lowers the CO_2 emission rate by 7.09% and 6.72% in the cases of MeOH : EtOH=3.5 : 1 and 1 : 3.5 concurrently with the reduced trend in TAC. The bottom temperature of the fuel ether separation column is low enough to use LP steam. Since LP steam has a smaller effect on CO_2 emissions than HP or MP steam, the outcome did not lead to a substantial reduction in the CO_2 emission rate in comparison to TAC. Compared to the bare individual production system, the CO_2 emission rate of the external HI individual production system exhibited a reduction of 6.52% and 10.5% for the MeOH : EtOH= 3.5 : 1 and 1 : 3.5 cases. As the required capital cost in the individual system was high, the CO_2 emission rate decreased more significantly compared to the TAC.

CONCLUSION

This study investigated the production of fuel ethers in both individual and co-production systems, where the reaction and separation processes were integrated using a mixed alcohol feed. Since the alcohol mixture in the actual production sites can be obtained in a wide range of compositional variations, simulations were conducted by varying the feed ratio of MeOH to EtOH for each system. Based on the TUC analysis, it was found that the co-production system offers a more energy-efficient design for the MeOH-dominant feed, while the EtOH-dominant feed favors the individual RD production system. This difference is mainly due to higher relative volatility of the alcohol pre-separation column and unfavorable reaction equilibrium for ETBE production in the EtOH excess case. Thus, when the MeOH portion is higher, the heat duty of the alcohol pre-separation column increases. Conversely, in the co-production system with an EtOH dominant feed, the higher internal flowrate of the fuel ether co-production column for the given same ETBE yield contributes to lower energy efficiency. When the MeOH flowrate is equal to the EtOH flowrate, the difference in TUC is negligible. This tendency is also reflected in the TAC and CO_2 emission rate. Moreover, the introduction of the external HI method further reduces the TUC, TAC, and CO_2 emissions. This reduction is achieved by minimizing the reboiler heat duty in the separation column through heat exchange between the bottom liquid and the hot product streams. The external HI co-production system has a lower recycle flowrate than external HI individual production system, leading to higher reduction in TUC. In addition to the drop in energy consumption, economical and eco-conscious alternatives are designed followed by the reboiler heat duty reduction.

ACKNOWLEDGEMENTS

This work was performed under the financial support from the ERC Center (NRF2022R1A5A1033719) and the Lotte Chemical-KAIST Carbon Neutrality R&D Center.

SUPPORTING INFORMATION

Additional information as noted in the text. This information is available via the Internet at http://www.springer.com/chemistry/journal/11814.

REFERENCES

1. W. W. Seo, J. H. Yim, J. S. Lim and K. Y. Choi, *Korean J. Chem. Eng.*, **39**, 3422 (2022).
2. A. Iqbal, M. A. Qyyum, Ojasvi, A. S. Nizami, S. A. Ahmad and M. Lee, *Chem. Eng. Process.: Process Intensif.*, **163**, 108376 (2021).
3. H. Lee, C. Seo, M. Lee and J. W. Lee, *AIChE J.*, **68**(1), e17476 (2022).
4. F. Qasim, J. S. Shin and S. J. Park, *Korean J. Chem. Eng.*, **35**, 1185 (2018).
5. J. Park, W. Lee and J. W. Lee, *Korean J. Chem. Eng.*, **40**, 46 (2023).
6. C. Seo, H. Lee, M. Lee and J. W. Lee, *Korean J. Chem. Eng.*, **39**, 263 (2022).
7. J. W. Lee, S. Hauan, K. M. Len and A. W. Westerberg, *Proc. R. Soc. Lond. A.*, **456**, 1953 (2000).
8. J. W. Lee, S. Hauan, K. M. Lien and A. W. Westerberg, *Proc. R. Soc. Lond. A.*, **456**, 1965 (2000).
9. M. Errico, C. Madeddu, M. Flemming Bindseil, S. Dall Madsen, S. Braekevelt and M. S. Camilleri-Rumbau, *Chem. Eng. Process.: Process Intensif.*, **157**, 108110 (2020).
10. J. W. Lee, S. Hauan and A. W. Westerberg, *Ind. Eng. Chem. Res.*, **39**, 1061 (2000).
11. F. J. Novita, H. Y. Lee and M. Lee, *Korean J. Chem. Eng.*, **35**, 926 (2018).

12. H. Lee, W. Jang and J. W. Lee, *Korean J. Chem. Eng.*, **36**, 954 (2019).
13. H. Mo, H. Lee, W. Jang, K. Namgung and J. W. Lee, *Korean J. Chem. Eng.*, **38**, 195 (2021).
14. V. D. Talnikar and Y. S. Mahajan, *Korean J. Chem. Eng.*, **31**, 1720 (2014).
15. S. H. Lee, W. Y. Choi, K. J. Kim, D. J. Chang and J. W. Lee, *Chem. Eng. Process.: Process Intensif.*, **123**, 249 (2018).
16. S. Ghosh and S. Srinivas, *Korean J. Chem. Eng.*, **39**, 2291 (2022).
17. R. Muthia, A. G. T. Reijneveld, A. G. J. van der Ham, A. J. B. ten Kate, G. Bargeman, S. R. A. Kersten and A. A. Kiss, *Chem. Eng. Process.: Process Intensif.*, **128**, 263 (2018).
18. K. Namgung, H. Lee, W. Jang, H. Mo and J. W. Lee, *Chem. Eng. Process.: Process Intensif.*, **154**, 108048 (2020).
19. J. W. Lee and A. W. Westerberg, *AIChE J*, **47**, 1333 (2001).
20. M. Carrera-Rodríguez, J. G. Segovia-Hernández and A. Bonilla-Petriciolet, *Ind. Eng. Chem. Res.*, **50**, 10730 (2011).
21. K. Huang, S. J. Wang and W. Ding, *Chem. Eng. Sci.*, **63**, 2119 (2008).
22. A. Norkobilov, D. Gorri and I. Ortiz, *Chem. Eng. Process.: Process Intensif.*, **122**, 434 (2017).
23. K. Zhou, Q. G. Zhang, G. L. Han, A. M. Zhu and Q. L. Liu, *J. Membr. Sci.*, **448**, 93 (2013).
24. M. Dahmen and W. Marquardt, *Energy Fuels*, **30**, 1109 (2016).
25. R. K. Saluja, V. Kumar, R. Sham, R. Kaushal and F. Inambao, *Advancement in oxygenated fuels for sustainable development*, Elsevier (2023).
26. Y. Chen, Q. Zhang, K. Liu, S. Zhang, X. Zhang and H. Liu, *Process Saf. Environ. Prot.*, **171**, 607 (2023).
27. K. Atsonios, K. D. Panopoulos and E. Kakaras, *Int. J. Hydrogen Energy*, **41**, 792 (2016).
28. R. L. Maglinao and B. B. He, *Ind. Eng. Chem. Res.*, **50**, 6028 (2011).
29. W. Jang, K. Namgung, H. Lee, H. Mo and J. W. Lee, *Ind. Eng. Chem. Res.*, **59**, 1966 (2020).
30. Y. C. Wu, H. Y. Lee, C. Y. Tsai, H. P. Huang and I. L. Chien, *Comput. Chem. Eng.*, **57**, 63 (2013).
31. A. Rehfinger and U. Hoffmann, *Chem. Eng. Sci.*, **45**, 1605 (1990).
32. Y. Tian, I. Pappas, B. Burnak, J. Katz and E. N. Pistikopoulos, *Chem. Eng. Sci.*, **230**, 116232 (2021).
33. R. Khaledi and B. R. Young, *Ind. Eng. Chem. Res.*, **44**, 3134, (2005).
34. R. Khaledi and P. R. Bishnoi, *Ind. Eng. Chem. Res.*, **45**, 6007 (2006).
35. J. B. Rasmussen, S. S. Mansouri, X. Zhang, J. Abildskov and J. Kjøbsted Huusom, *Chem. Eng. Process.: Process Intensif.*, **167**, 108843 (2021).
36. A. Iftakher, D. A. Liñán, S. S. Mansouri, A. Nahid, M. M. F. Hasan, M. A. A. S. Choudhury, L. A. Ricardez-Sandoval and J. H. Lee, *Comput. Chem. Eng.*, **164**, 107869 (2022).
37. B. H. Bisowarno, Y. C. Tian and M. O. Tadé, *Chem. Eng. J.*, **99**, 35 (2004).
38. C. Thiel, K. Sundmacher and U. Hoffmann, *Chem. Eng. J.*, **66**, 181 (1997).
39. H. Lee, H. Mo, K. Namgung, W. Jang and J. W. Lee, *Ind. Eng. Chem. Res.*, **59**, 14398 (2020).
40. Z. Guo, M. Ghufran and J. W. Lee, *AIChE J*, **49**, 3161 (2003).
41. J. Chin, H. J. Kattukaran and J. W. Lee, *Ind. Eng. Chem. Res.*, **43**, 7092 (2004).
42. Y. Xu, J. Li, Q. Ye and Y. Li, *Sep. Purif. Technol.*, **277**, 119498 (2021).
43. X. You, I. Rodriguez-Donis and V. Gerbaud, *Appl. Energy*, **166**, 128 (2016).
44. D. Jantes-Jaramillo, J. G. Segovia-Hernández and S. Hernández, *Chem. Eng. Technol.*, **31**, 1462 (2008).
45. M. A. Gadalla, Z. Olujic, P. J. Jansens, M. Jobson and R. Smith, *Environ. Sci. Technol.*, **39**, 6860 (2005).
46. M. Gadalla, Ž. Olujić, M. Jobson and R. Smith, *Energy*, **31**, 2398 (2006).
47. M. Lee, H. Lee, C. Seo, J. Lee and J. W. Lee, *Sep. Purif. Technol.*, **287**, 120598 (2022).
48. A. Anbreen, N. Ramzan and M. Faheem, *Chem. Eng. Process.: Process Intensif.*, **170**, 108695 (2022).
49. Y. Zhuang, Y. Xing, L. Zhang, L. Liu, J. Du and S. Shen, *Comput. Chem. Eng.*, **152**, 107388 (2021).

Supporting Information

Elevated energy efficiency and reduced CO_2 emissions from integrated reaction and separation for the concurrent production of ethers

Jeongwoo Lee, Minyong Lee, Donggun Kim, Yongbeom Shin, and Jae W. Lee†

Department of Chemical and Biomolecular Engineering, Korea Advanced Institute of Science and Technology (KAIST), 291 Daehak-ro, Yuseong-gu, Daejeon 34141, South Korea
(*Received 4 August 2023 • Revised 4 September 2023 • Accepted 5 September 2023*)

Table S1. Binary interaction coefficient for UNIQUAC method

Component i	Component j	b_{ij}	b_{ji}	Reference
ETBE	EtOH	−102.322	424.521	[1]
ETBE	IB	39.215	−21.484	[1]
ETBE	MeOH	−491.524	47.725	*
ETBE	MTBE	20.627	−26.031	*
ETBE	NB	42.130	−20.041	[1]
EtOH	IB	436.034	−46.937	[1]
EtOH	MeOH	31.43456	−81.5779	*
EtOH	MTBE	20.62741	−26.0312	*
EtOH	NB	404.721	−26.930	[1]
IB	MeOH	−706.267	35.37638	[2]
IB	MTBE	−52.1988	24.62296	[2]
IB	NB	24.245	−23.894	[1]
MeOH	MTBE	88.03297	−468.712	[2]
MeOH	NB	7.358646	−731.533	*
MTBE	NB	22.95032	−51.1891	[2]

* UNIFAC estimation

Table S2. TUC comparison of the designed systems of all alcohol feed ratios (Unit: kW)

MeOH : EtOH	Individual production	External HI individual production	Co-production	External HI co-production
3.5 : 1	14,476.75	13,987.63	9,908.86	9,191.86
3 : 1	14,374.73	13,957.99	9,243.18	8,768.78
2 : 1	11,894.85	11,387.96	8,757.78	8,147.85
1 : 1	9,428.56	9,025.58	9,285.49	8,690.93
1 : 2	9,107.45	8,657.14	9,399.26	8,722.67
1 : 3	9,050.63	8,640.35	9,536.75	8,917.43
1 : 3.5	8,743.13	8,227.62	9,633.62	8,946.27

Table S3. Condenser and reboiler heat duty of alcohol separation column in whole cases (Unit: kW)

MeOH : EtOH	3.5 : 1	3 : 1	2 : 1	1 : 1	1 : 2	1 : 3	1 : 3.5
Condenser	−5,694.77	−5,382.83	−4,579.38	−3,327.22	−2,895.12	−2,755.46	−2,723.48
Reboiler	5,774.75	5,465.92	4,672.06	3,439.49	3,028.61	2,899.78	2,871.45
Heat duty	11,469.53	10,848.75	9,251.44	6,766.71	5,923.73	5,655.24	5,594.93

Table S4. TUC comparison of the designed systems when MeOH : EtOH=3.5 : 1 (Unit: kW)

	Individual production	External HI individual production	Co-production	External HI co-production
C1				
Condenser	−5,694.77	−5,694.77	−2,758.67	−2,758.67
Reboiler	5,774.75	-	2,291.93	2,291.93
C2				
Condenser	−1,392.72	−1,392.72	−2,845.44	−2,486.94
Reboiler	989.53	989.53	2,012.81	-
C3				
Condenser	−285.92	−285.92	-	-
Reboiler	323.82	323.82	-	-
The others	Two pumps 15.24	Two pumps Auxiliary heater 5,300.87	Pump 12.217	Pump Auxiliary heater 1,654.32
TUC	14,476.75	13,987.63	9,908.86	9,191.86

Table S5. TUC comparison of the designed systems when MeOH : EtOH=1 : 1 (Unit: kW)

	Individual production	External HI individual production	Co-production	External HI co-production
C1				
Condenser	−3,327.22	−3,327.22	−2,525.05	−2,525.05
Reboiler	3,439.49		2,349.31	2,349.31
C2				
Condenser	−812.02	−812.02	−2,624.11	−2,326.80
Reboiler	621.58	621.58	1,774.58	-
C3				
Condenser	−619.64	−619.64	-	-
Reboiler	593.07	593.07	-	-
The others	Two pumps 15.535	Two pumps Auxiliary heater 3,052.05	Pump 12.448	Pump Auxiliary heater 1,489.77
TUC	9,428.56	9,025.58	9,285.49	8,690.93

Table S6. TUC comparison of the designed systems when MeOH : EtOH=1 : 3.5 (Unit: kW)

	Individual production	External HI individual production	Co-production	External HI co-production
C1				
Condenser	−2,723.48	−2,723.48	−2,811.39	−2,811.39
Reboiler	2,871.45	-	2,515.70	2,515.70
C2				
Condenser	−396.15	−396.15	−2,520.07	−2,176.40
Reboiler	387.68	387.68	1,773.95	-
C3				
Condenser	−1,226.95	−1,226.95		
Reboiler	1,121.72	1,121.72		
The others	Two pumps 15.551	Two pumps Auxiliary heater 2,371.49	Pump 12.507	Pump Auxiliary heater 1,430.27
TUC	8,743.13	8,227.62	9,633.62	8,946.27

Table S7. Reflux ratio of RD column in co-production system

MeOH : EtOH	3.5 : 1	3 : 1	2 : 1	1 : 1	1 : 2	1 : 3	1 : 3.5
Reflux ratio	3.48	3.60	3.77	4.15	4.82	5.31	5.76

Table S8. Parameters for analyzing economics [3]

	Column vessel (Diameter and length in m)
	Diameter and length: obtained by Aspen Plus Economic Analyzer Capital cost=17640(diameter)$^{1.066}$(length)$^{0.802}$
	Condenser (area in m^2)
	Heat transfer coefficient=0.852 kW/(K·m^2) Pinch temperature=13.9 K Capital cost=7296(area)$^{0.65}$
	Reboiler (area in m^2)
	Heat transfer coefficient=0.568 kW/(K·m^2) Pinch temperature=34.8 K Capital cost=7296(area)$^{0.65}$
	Energy cost
	Chilled water (5 °C)=$4.43/GJ LP steam (6 bar, 160 °C)=$7.78/GJ MP steam (11 bar, 184 °C)=$8.22/GJ HP steam (42 bar, 254 °C)=$9.88/GJ

Table S9. Parameters for calculating CO_2 emission rate [4]

Parameters	Description		Value	Unit
λ_{Proc}	Latent heat of steam delivered to the process	LP steam (6 bar)	2,085.766	kJ/kg
		MP steam (11 bar)	1,999.621	
		HP steam (42 bar)	1,698.075	
h_{Proc}	Enthalpy of steam delivered to the process	LP steam (6 bar)	2,756.143	
		MP steam (11 bar)	2,780.648	
		HP steam (42 bar)	2,799.786	
T_{Stack}	Stack temperature	LP steam (6 bar)	160	°C
		MP steam (11 bar)	184	
		HP steam (42 bar)	254	
T_{FTB}	Flame temperature		1,800	°C
T_0	Ambient temperature		25	°C
α	Ratio of molar masses of CO_2		3.67	-
NHV	Net heating value		39,771	kJ/kg
C	Carbon content		86.5	%

Table S10. Calculated heat of each product streams of all alcohol feed ratios (Unit: kJ)

MeOH : EtOH	MTBE stream	ETBE stream	Chosen stream
3.5 : 1	1.557e+6	7.208e+5	MTBE
3 : 1	1.502e+6	8.065e+5	MTBE
2 : 1	1.330e+6	1.077e+6	MTBE
1 : 1	9.947e+5	1.611e+6	ETBE
1 : 2	6.636e+5	2.153e+6	ETBE
1 : 3	4.975e+5	2.420e+6	ETBE
1 : 3.5	4.424e+5	2.504e+6	ETBE

Criteria for selecting product stream in external HI individual production system

Two product streams, ETBE stream and MTBE stream are able to exchange heat with the liquid stream coming from the last stage of alcohol separation column. High content of heat is able to transfer heat to the cold stream, leading to further reduction in auxiliary heater duty requirement. Selecting the stream is based on the heat amount contained in the hot stream. Transferable heat amount is calculated as following:

$$Q=C_p \times n \times \Delta T$$

where C_p denotes the heat capacity of the mixture (kJ/K/kmol), n denotes the molar flowrate (kmol), and ΔT denotes the temperature difference between hot and minimum temperature that hot stream could reach, which is the sum of minimum temperature difference and cold stream temperature (K). MTBE stream was selected in the methanol excess cases, and ETBE stream was selected in the other cases. Calculated heat of each product streams is shown in Table S10.

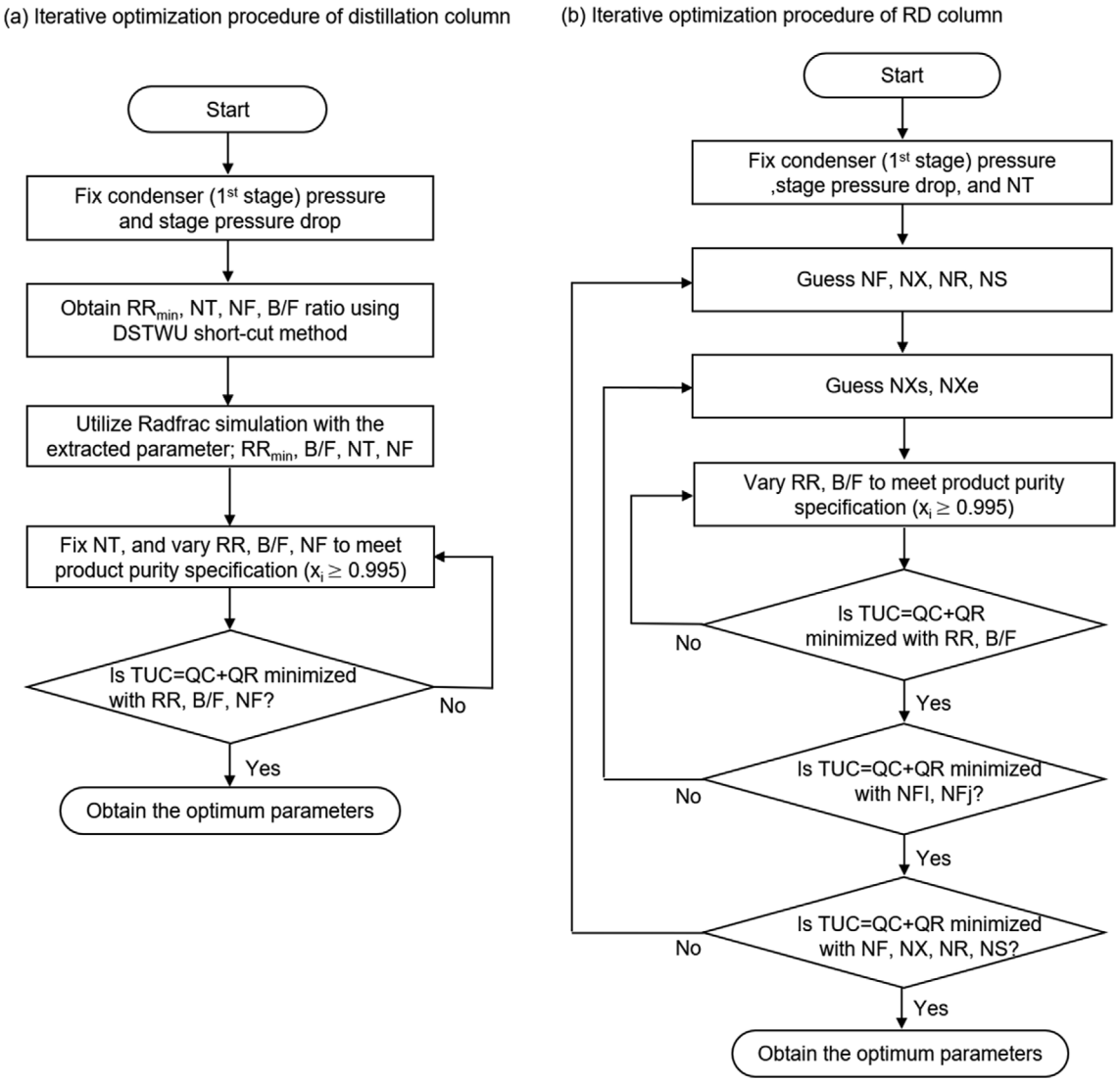

Fig. S1. Iterative optimization procedure of (a) distillation column, (b) RD column.

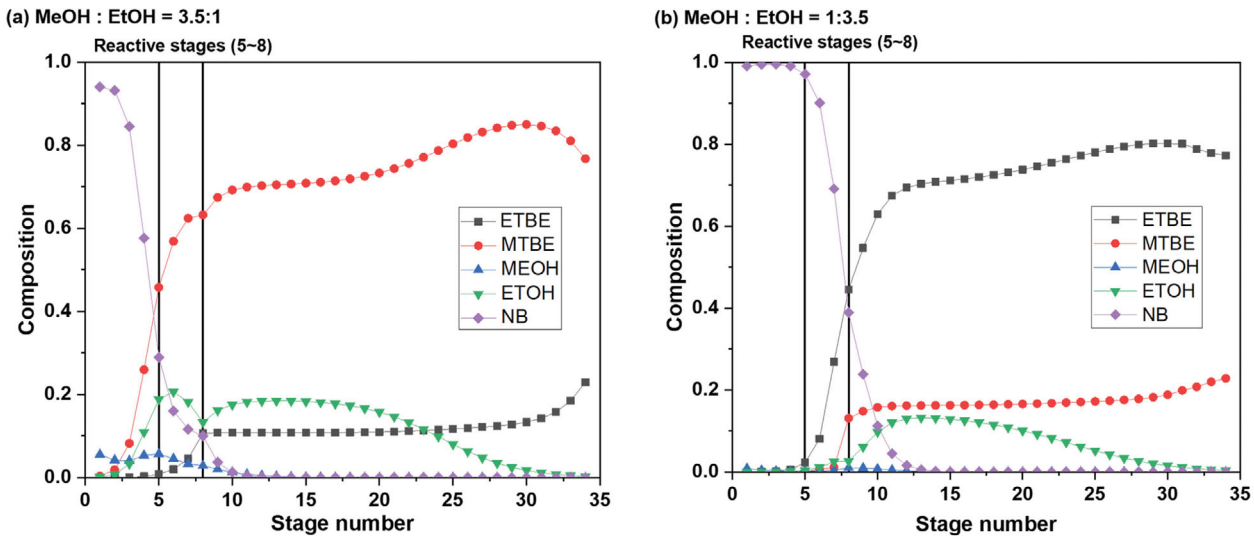

Fig. S2. Liquid phase profile of the fuel ether co-production column in the case of (a) MeOH : EtOH=3.5 : 1, (b) MeOH : EtOH=1 : 3.5.

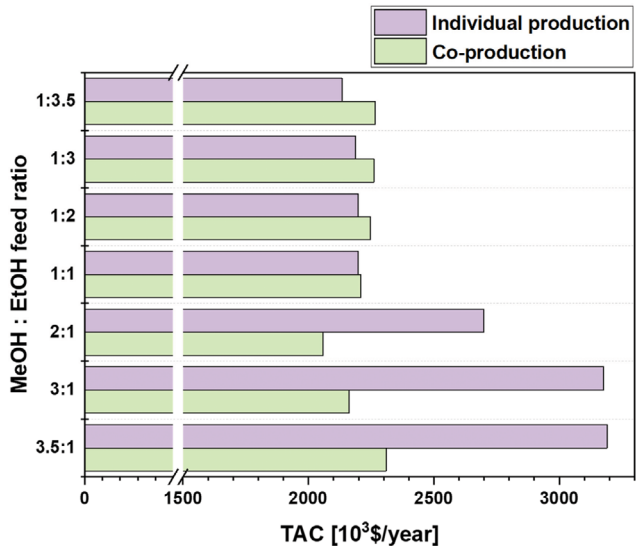

Fig. S3. TAC comparison of all alcohol feed ratio cases.

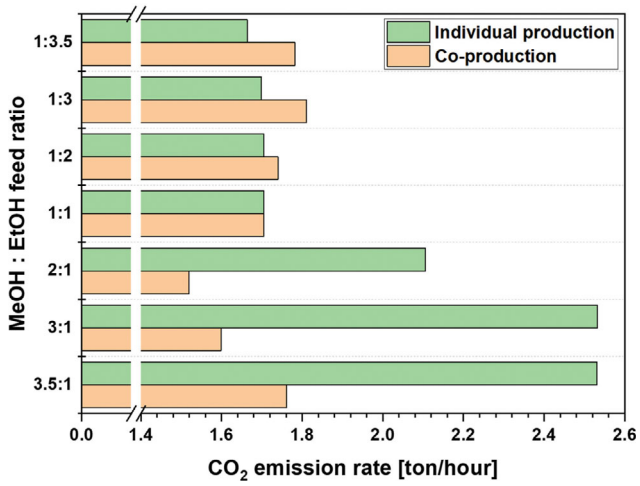

Fig. S4. CO_2 emission rate comparison of all alcohol feed ratio cases.

REFERENCES

1. R. Khaledi and P. R. Bishnoi, *Ind. Eng. Chem. Res.*, **45**, 6007 (2006).
2. A. Rehfinger and U. Hoffmann, *Chem. Eng. Sci.*, **45**, 1605 (1990).
3. W. L. Luyben, Distillation Design and Control Using AspenTM Simulation, Second Edition, John Wiley & Sons: Inc: New York (2013).
4. M. Gadalla, Ž. Olujić, M. Jobson and R. Smith, *Energy*, **31**, 2398 (2006).